

ORIGINAL RESEARCH

Open Access

Lithium ion intercalation mechanism for LiCoPO_4 electrode

Hua Ju¹, Jun Wu² and Yanhui Xu^{2*}

Abstract

Recently, there exists a discrepancy on the lithium ion de-intercalation mechanism for LiCoPO_4 electrode. In the present work, the study was focused upon exploring the origin of this discrepancy by studying the dependence of the impedance spectrum on the state of charge and the carbon content. For the pure LiCoPO_4 electrode, the two plateaus in the charge curve are at 4.82 and 4.92 V. We have also studied the variation of electrochemical impedance spectroscopies (EISs) with the state of charge. The EIS measurement has shown that the total interfacial resistance increases as the state of charge increases for the pure LiCoPO_4 electrode. If higher content of sucrose was added in the precursor (this implies higher carbon content in the synthesized sample), only one potential plateau can be found in the charge curve. For this electrode, the total interfacial resistance decreases with the state of charge. Especially, the total interfacial resistance has a dramatic decrease when the state of charge increases from 20% to 40%. It is believed that the influence of carbon impurity on the variation tendency of the EIS pattern may reflect the change of the fine structure. For the pure LiCoPO_4 electrode, the intermediate phase is $\text{Li}_{0.20-0.45}\text{CoPO}_4$.

Keywords: Electrochemical impedance spectroscopy, Interfacial resistance, Olivine phosphate, Lithium ion de-intercalation

Background

The growing crisis in energy and resource encourages scientists to search for various solutions [1-4], and in the past decades, much more attention has been paid on the research and development of lithium-ion batteries, especially the cathode and anode materials [5-8]. Among them, the olivine-type LiCoPO_4 cathode has been extensively studied due to its highly reversible Li-intercalation potential of 4.7 to 4.8 V [9-13]. Due to the expensive cost of Co sources, LiCoPO_4 is not suitable for large-scale applications, but it has a potential in lithium-ion microbattery and all-solid-state lithium-ion battery. In addition, the understanding of the electrochemical behavior of LiCoPO_4 is also useful to improve the electrode properties of LiFePO_4 and LiMnPO_4 cathodes.

The density of cubic olivine LiCoPO_4 is reported to be 3.76 g cm^{-3} . Its structure can transit from the olivine-type to the spine-type structure as the atmosphere pressure

increases up to about 20 GPa. The single-crystal LiCoPO_4 is of dark purple color [14], with $a = 1.02 \text{ nm}$, $b = 0.59 \text{ nm}$, and $c = 0.47 \text{ nm}$. Cell parameters a and b increase but parameter c decreases as the x value increases for Li_xCoPO_4 . The unit cell volume becomes larger with the lithium ion content [15]. The room-temperature conductivity is in the order of magnitude of $10^{-10} \text{ S cm}^{-1}$, and the conduction activation energy is reported to be 0.51 eV by Ruffo et al. [16] and 0.62 eV by Rissouli et al. [17]. Impurity is a crucial factor affecting its conductivity [18]; the partial substitution of Co by Cr or Cu can give a conductivity of about $10^{-4} \text{ S cm}^{-1}$. Ehrenberg et al. [19] proposed a three-phase reaction mechanism including LiCoPO_4 , Li_zCoPO_4 ($z = 0.6$ to 0.7), and Li_yCoPO_4 . The subscript 'y' approaches zero but does not equal to zero.

Until now, the reaction mechanism of LiCoPO_4 remains controversial. The reported charge curves are somewhat different. In the report by Yamada and Chung [20], only one potential plateau can be found, while Bramnik et al. [15] and Ruffo et al. [16] reported two potential plateaus in the charging curve. It is believed that there must be some reasons leading to the discrepancy. The solution of

* Correspondence: xuyanhui@suda.edu.cn

²Institute of Chemical Power Sources, Soochow University, Suzhou 215006, People's Republic of China

Full list of author information is available at the end of the article

the discrepancy will promote the understanding of the electrochemical behavior of all the olivine-type phosphates. In this work, we measured the impedance response of the LiCoPO_4 electrode with different states of charge and tried to explore the lithium ion intercalation reaction mechanism.

Methods

The samples were synthesized by a high-temperature solid-state reaction method. The mixture of $\text{CH}_3\text{COOLi}\cdot\text{H}_2\text{O}$, $(\text{CH}_3\text{COO})_2\text{Co}\cdot 4\text{H}_2\text{O}$, and $\text{NH}_4\text{H}_2\text{PO}_4$ (1.05:1:1, mol/mol/mol) and sucrose (0, 2, 5, 8, and 10 wt.%) were firstly dissolved in distilled water, preheated in N_2 atmosphere for 3 h at 300°C , and then ball-milled for 4 h to ensure homogeneous mixing. At last, the precursor was heated in N_2 for 20 h at 700°C . It is believed that all the prepared samples contained carbon impurity because the raw chemicals contain the element carbon. Therefore, the pure LiCoPO_4 having no carbon impurity was synthesized by heating the mixture of $\text{CH}_3\text{COOLi}\cdot\text{H}_2\text{O}$, $(\text{CH}_3\text{COO})_2\text{Co}\cdot 4\text{H}_2\text{O}$, and $\text{NH}_4\text{H}_2\text{PO}_4$ (1.05:1:1, mol/mol/mol) in air atmosphere.

X-ray diffraction (Rigaku IV, Shibuya-ku, Japan) with $\text{Cu K}\alpha$ radiation was performed to identify the phase structure. The applied voltage and current were 40 kV and 50 mA, respectively. The electrode was made of the mixture of active mass, a conductive additive (SuperP, Timcal, Bodio, Switzerland), and a binder (PVDF) in a weight ratio of 8:1:1. The mixture slurry was cast on an Al foil current collector. The loading of the active mass was 3 to 6 mg cm^{-2} . For the charge–discharge measurement, a 2016-type coin cell was used by assembling it in an argon-filled glove box with lithium metal as the counter electrode. The electrolyte was 1 M $\text{LiPF}_6/\text{EC} + \text{DEC}$ (v/v , 1:1). A laboratory-made three-electrode compartment was used to carry out the electrochemical impedance measurement. A lithium metal electrode was used as the reference and the counter electrode. The charge–discharge test was carried out on a LAND CT 2001A system (Wuhan Jinnuo Electronics Co. Ltd., Wuhan, China), and the electrochemical impedance spectroscopy (EIS) test was performed on PE Parc 2273 (Princeton Applied Research, Oak Ridge, TN, USA) or CHI660C (CH Instruments Inc., Austin, TX, USA) electrochemical workstations. The amplitude of the applied voltage signal was 5 mV.

Results and discussion

Figure 1 shows the X-ray diffraction patterns of the as-prepared samples. The main phase is found to be a cubic olivine-type LiCoPO_4 with $a = 0.5699$ nm, $b = 1.021$ nm, and $c = 0.458$ nm. The crystallographic structure is not influenced by the carbon addition. When the content of added sucrose is more than 8 wt.%, the diffraction peaks of the Co_2P phase become more obvious. No

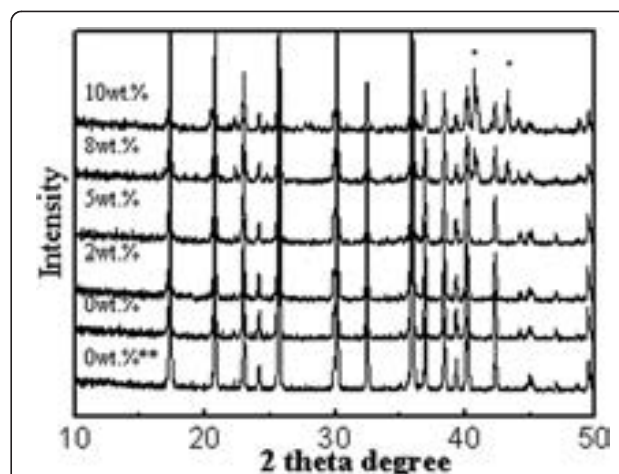


Figure 1 The X-ray diffraction patterns of the samples with different amounts of added sucrose. The '0 wt.%**' indicates that the sample was synthesized in air atmosphere, and others were synthesized in N_2 atmosphere. The diffraction peaks with asterisk are the Co_2P phase.

other impurity phase can be detected by the X-ray diffraction (XRD) technique. According to the Scherrer equation, the average particle size is calculated to be about 130 nm for all the samples. Adding sucrose into the precursor did not obviously affect the particle size.

It could be plausibly concluded that the sample synthesized in air atmosphere is of pure olivine-type structure and does not contain any impurity including carbon and Co_2P phase, and this sample is denoted as LCP-1 while other samples with 0, 2, 5, 8 and 10 wt.% sucrose added in the precursor are denoted as LCP-2, LCP-3, LCP-4, LCP-5, and LCP-6, respectively, for a convenient description. Figure 2 shows the transmission electron microscopy (TEM) images of two typical samples: LCP-1 and LCP-6. The particle is of round shape, and its size is about 175 nm in diameter. The particle size is found not to be affected by the sucrose addition and larger than that calculated from the XRD data, which was calculated by the Scherrer equation. The Scherrer equation is accurate only when the particle size is in the range of 10 to 100 nm. From Figure 2, it can still be found that the surface carbon film is about 5 nm in thickness. For the pure sample, there is no surface carbon film found.

Figure 3 shows the dependence of the dQ/dV on voltage for the two typical LiCoPO_4 electrodes: LCP-1 and LCP-6. For the pure LiCoPO_4 electrode (LCP-1), there exist two potential plateaus in the charge curve, while for the LCP-6, there exists only one potential plateau in the charge curve. There is only one potential plateau in the discharge curve, which is independent of the amount of the added sucrose in the precursor. The two charge potential plateaus position at 4.82 and 4.92V, respectively, as indicated by the two arrows. The charge capacity of the

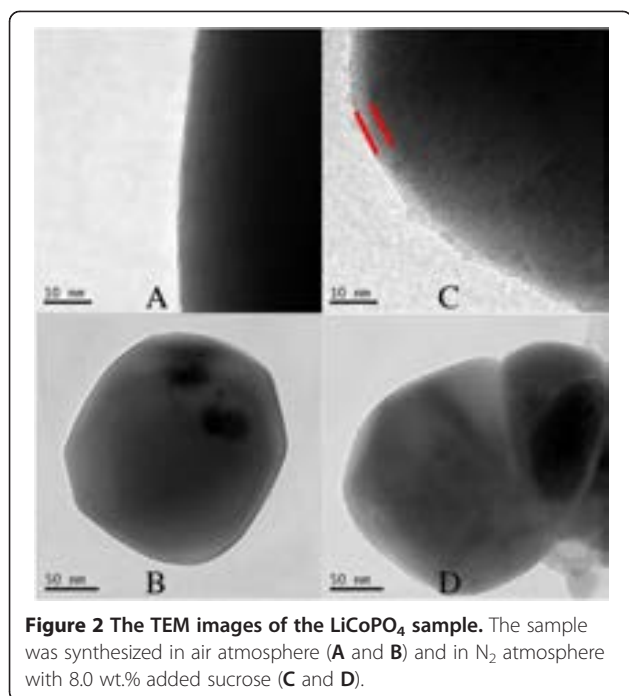


Figure 2 The TEM images of the LiCoPO_4 sample. The sample was synthesized in air atmosphere (A and B) and in N_2 atmosphere with 8.0 wt.% added sucrose (C and D).

4.82-V plateau is about 20% of the total capacity, while that of the 4.92-V plateau is about 55% of the total capacity. The transition between the first plateau and the second one can be found, as shown in Additional file 1: Figure S1. The discharge potential plateau is about 4.70 V. For samples with more sucrose added in the precursor, during charging, their potential increases rapidly up to 5.0 V. The discharge potential plateau shifts towards a more negative potential and is about 4.5 V. The difference between charge and discharge potentials becomes larger, which may imply that higher carbon content will make the electrochemical reaction less reversible.

Figure 4 shows the impedance spectra of the electrodes made of the LCP-1 and LCP-6 samples at different states of charge. It can be seen from Figure 4A that the EIS pattern exhibits a dramatic variation as the state of charge decreases from 40% to 20%. The size of the semicircle suddenly increases from about 100 Ω in the state of charge (SOC) of more than 40% to about 300 Ω in the SOC of less than 40% for the LCP-1 electrode. However, for the LCP-6 electrode, the variation of the impedance spectroscopy pattern with the SOC is relatively smooth, as shown in Figure 4B.

The explanation of the physical meaning of the semicircle in the EIS Nyquist plot remains controversial. Fewer researchers preferred that the semicircle represents the contact resistance between the collector and the active material particles. However, most researchers accepted the conclusion that it corresponds to the response of the interface between lithium insertion electrode and liquid electrolyte [21-23]. In the present work,

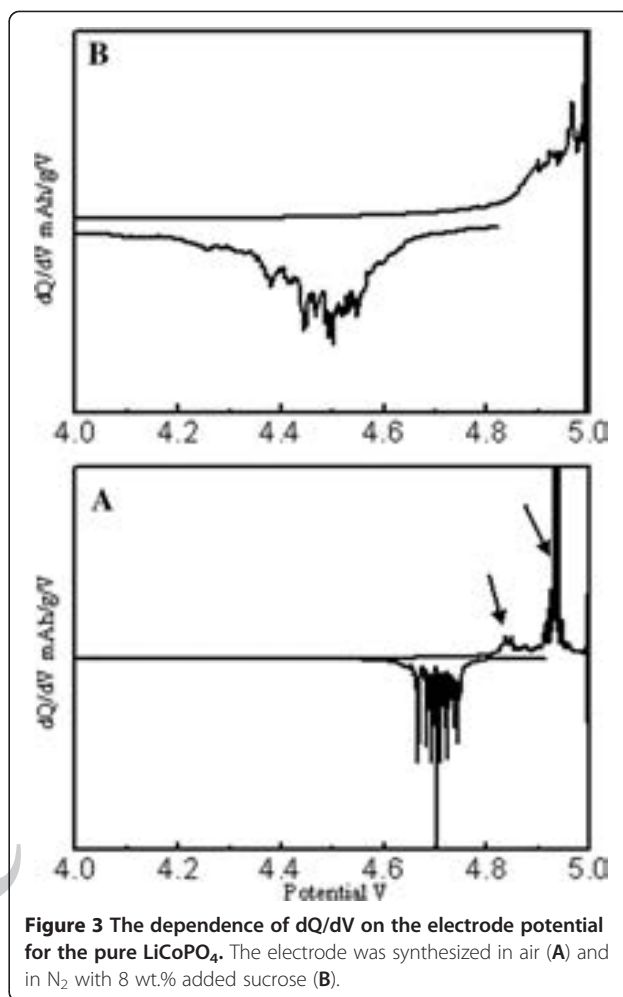
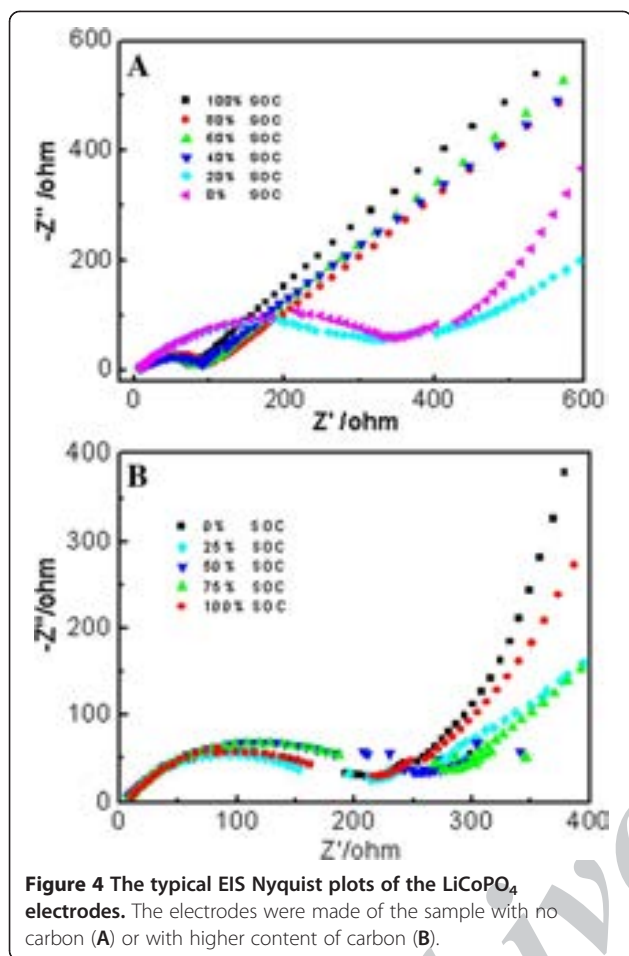


Figure 3 The dependence of dQ/dV on the electrode potential for the pure LiCoPO_4 . The electrode was synthesized in air (A) and in N_2 with 8 wt.% added sucrose (B).

it is accepted that it represents the total interface resistance being in parallel with the interfacial capacitance. According to the equation [24]

$$Y_0^n R_{ct}^{\frac{1}{n}} \sin\left(\frac{n\pi}{2}\right) = R_{ct} C_{dl},$$

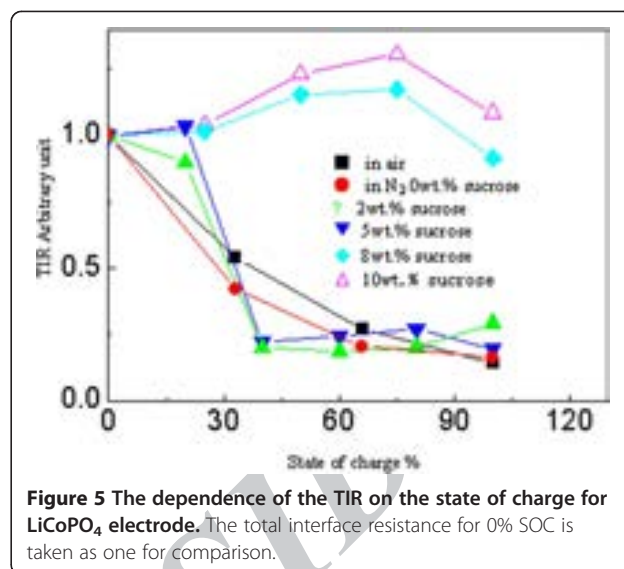
the total interfacial capacitance is calculated to be 0.5 to 0.9 $\mu\text{F cm}^{-2}$, which is consistent with the report [21]. Here the parameters Y_0 , n , and R_{ct} can be obtained by fitting the EIS data using the EQUIVCRT software. The dependence of the total interface resistance on the states of charge is shown in Figure 5, where the total interfacial resistance (TIR) value of the electrode with 0% SOC is arbitrarily taken as one, the reference value. Here the variation tendency of the TIR vs. SOC is of more importance. The dependence of the TIR on the SOC may provide some useful information on the microstructure or the crystallographic structure, as well as on the nature of the two potential plateaus for the LiCoPO_4 with lower carbon content and the single potential plateau for the LiCoPO_4 with higher carbon content. It is clear from Figure 5 that the electrode has a relatively smaller TIR



in the higher SOC when the amount of the added sucrose is relatively small. Here it is reasonable to conclude that a higher amount of added sucrose in the precursor should correspond to higher carbon content in the product. In contrast, for the sample with higher carbon content, the electrode has a relatively larger TIR in the higher SOC. For the LCP-1 to LCP-4 electrodes, the TIR has a dramatic decrease as the state of charge increases from 20% to 40%. For the LCP-5 and LCP-6 electrodes, the TIR has a tendency to increase as the state of charge increases.

The quantitative, even qualitative, explanation of the obtained EIS pattern is still difficult, but it is still believed that the dependence of EIS on the SOC and carbon content is related with the shape of the charge curves, at least it can provide some useful information on its nature.

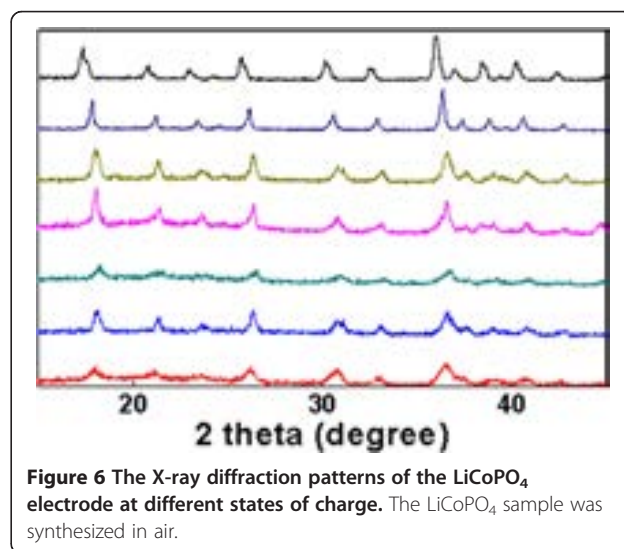
As mentioned above in the 'Background' section, there is a discrepancy on the Li-de-intercalation reaction mechanism of the LiCoPO_4 electrode. Some literatures reported a two-plateau charge curve, and others reported a single-plateau charge curve, in which the electrode potential increased rapidly up to 5.0 V. In the present work, the influence of the different carbon contents on the charge



curves has been examined and representative results are presented. It is believed that the present results are valuable. Here the Co_2P phase may thus also have a contribution. A synergistic effect is also possible.

In principle, the XRD analysis may be useful to determine the nature of the charge curve and to solve the discrepancy via studying the dependence of the crystallographic structure on the state of charge. Figure 6 shows the XRD patterns of the pure LiCoPO_4 electrode. The electrodes were firstly cycled for five times and then used for XRD measurements. As the lithium ion de-intercalated, the volume of the unit cell becomes smaller, but the crystallographic structure remains unchanged.

However, the EIS measurements are successful. It is believed that the fine crystallographic structure should be different when the electrode is positioned at the two different potential plateaus. The reason for the



discrepancy on the Li-de-intercalation reaction mechanism seems likely to be solved based on our results. The carbon content in the samples is the crucial factor. For the pure LiCoPO_4 (LCP-1) and low-carbon-content LiCoPO_4 , the lithium de-intercalation proceeds via a three-phase mechanism, i.e., LiCoPO_4 , Li_xCoPO_4 , and Li_yCoPO_4 . Here the value of y remains unknown based on our results, but the value of x should be in the range of 0.20 to 0.45 based on the charge–discharge measurement. The results of the LiFePO_4/C sample [20] may also be effective to the LiCoPO_4/C electrode. When the carbon content becomes higher, the miscibility between the Li-poor and Li-rich phases becomes better, which leads to the change of the charge curve.

Conclusion

In the present work, the electrochemical impedance spectroscopy technique is used to analyze the Li de-intercalation mechanism of the LiCoPO_4 electrode. The shape of the charge curve depends on the carbon content. For the pure LiCoPO_4 and the LiCoPO_4 sample synthesized in N_2 atmosphere with lower content of sucrose added in the precursor, there exist two potential plateaus in the charge curve. Only one potential plateau can be found if a large amount of sucrose was added in the precursor. The EIS results have shown that the total interface resistance decreases as the state of charge increases for the sample without any impurity and with very low carbon content. In contrast, for the sample with larger carbon content, the total interface resistance has a tendency to increase as the state of charge increases. For the sample with relatively low carbon content, the lithium de-intercalation reaction proceeds via a three-phase mechanism. The intermediate phase should be Li_xCoPO_4 , where x is 0.20 to 0.45. The Co_2P phase may also have a contribution, and further in-depth investigation is necessary.

Additional file

Additional file 1: Figure S1. The charge–discharge curves of a typical LiCoPO_4 electrode made of the sample with low carbon content or no carbon.

Competing interests

The authors declare that they have no competing interests.

Authors' contributions

HJ proposed the research idea and participated in the design of the study. JW carried out the experiments. YX drafted the manuscript. All authors read and approved the final manuscript.

Acknowledgements

The work is supported by grant numbers BK2009110, 2010A610151, and 2009EG111014.

Author details

¹School of Urban Rail Transportation, Soochow University, Suzhou 215131, People's Republic of China. ²Institute of Chemical Power Sources, Soochow University, Suzhou 215006, People's Republic of China.

Received: 30 June 2012 Accepted: 17 April 2013

Published: 30 April 2013

References

1. Sharma, P, Harinarayana, T: Solar energy generation potential along national highways. *International Journal of Energy and Environmental Engineering* **4**, 16 (2013)
2. Andante, P, Hiroshi, O, Katsuya, N: Energy recovery potential and life cycle impact assessment of municipal solid waste management technologies in Asian countries using ELP model. *International Journal of Energy and Environmental Engineering* **3**, 28 (2012)
3. Kajsa, F, Åke, B, Marie-Claude, D: Low-energy office buildings using existing technology: simulations with low internal heat gains. *International Journal of Energy and Environmental Engineering* **3**, 19 (2012)
4. Li, PW, Ki, JP, Liu, H: Analysis and optimization of current collecting systems in PEM fuel cells. *International Journal of Energy and Environmental Engineering* **3**, 2 (2012)
5. Li, ZH, Ju, L, Li, DC, Zheng, JW, Xu, YH: The MMA and SO_3Li -grafted polypropylene separator used in Li ion batteries. *Ionics* **18**, 673–677 (2012)
6. Xu, GL, Chen, SR, Li, JT, Ke, FS, Huang, L, Sun, SG: A composite material of SnO_2 /ordered mesoporous carbon for the application in lithium-ion battery. *J. Electroanal. Chem.* **656**, 185–191 (2011)
7. Dong, YZ, Zhao, YM, Chen, YH, He, ZF, Kuang, Q: Optimized carbon-coated LiFePO_4 cathode material for lithium-ion batteries. *Mater. Chem. Phys.* **115**, 245–250 (2009)
8. Tarascon, JM, Armand, M: Issues and challenges facing rechargeable lithium batteries. *Nature* **414**, 359–367 (2001)
9. Han, DW, Kang, YM, Yin, RZ, Song, MS, Kwon, HS: Effects of Fe doping on the electrochemical performance of LiCoPO_4/C composites for high power-density cathode materials. *Electrochem. Comm.* **11**, 137–140 (2008)
10. Wolfenstine, J, Poesse, B, Allen, JL: Chemical oxidation of LiCoPO_4 . *J. Power. Sources* **138**, 281–282 (2004)
11. Kornev, I, Rivera, JP, Gentil, S, Jansen, AGM, Bichurin, M, Schmod, H, Wyder, P: Magnetolectric properties of LiCoPO_4 : microscopic theory. *Physica B* **271**, 304–308 (1999)
12. Kishore, MVMS, Varadaraju, UV: Influence of isovalent ion substitution on the electrochemical performance of LiCoPO_4 . *Mater. Res. Bull.* **40**, 1705–1712 (2005)
13. Huang, X, Ma, JF, Wu, PW, Hu, YM, Dai, JH, Zhu, ZB, Chen, HY, Wang, HF: Hydrothermal synthesis of LiCoPO_4 cathode materials for rechargeable lithium ion batteries. *Mater. Lett.* **59**, 578–582 (2005)
14. Martin, RS, Franger, S: Growth of LiCoPO_4 single crystals using an optical floating-zone technique. *J. Crystal Growth* **310**, 861–864 (2008)
15. Bramnik, NN, Bramnik, KG, Baehtz, C, Ehrenberg, H: Study of the effect of different synthesis routes on Li extraction–insertion from LiCoPO_4 . *J. Power. Sources* **145**, 74–81 (2005)
16. Ruffo, R, Mari, CM, Morazzoni, F, Rosciano, F, Scotti, R: Electrical and electrochemical behaviour of several $\text{LiFexCo}_{1-x}\text{PO}_4$ solid solutions as cathode materials for lithium ion batteries. *Ionics* **13**, 287–291 (2007)
17. Rissouli, K, Benkhoulja, K, Barrado, JRR, Julien, C: Electrical conductivity in lithium orthophosphates. *Mater. Sci. Eng.* **98**, B185–B189 (2003)
18. Wolfenstine, J: Electrical conductivity of doped LiCoPO_4 . *J. Power. Sources* **158**, 1431–1435 (2006)
19. Ehrenberg, H, Bramnik, NN, Senyshyn, A, Fuess, H: Crystal and magnetic structures of electrochemically delithiated $\text{Li}_{1-x}\text{CoPO}_4$ phases. *Solid State Sci.* **11**, 18–23 (2009)
20. Yamada, A, Chung, SC: Crystal chemistry of the olivine-type $\text{Li}(\text{MnyFe}_{1-y})\text{PO}_4$ and $(\text{MnyFe}_{1-y})\text{PO}_4$ as possible 4V cathode materials for lithium batteries. *J. Electrochem. Soc.* **148**, A960–A967 (2001)
21. Sauvage, F, Laffont, L, Tarascon, JM, Baudrin, E: Factors affecting the electrochemical reactivity vs. lithium of carbon-free LiFePO_4 thin films. *J. Power. Sources* **175**, 495–501 (2008)
22. Rahman, MM, Wang, JZ, Idris, NH, Chen, Z, Liu, HK: Enhanced lithium storage in a $\text{VO}_2(\text{B})$ -multiwall carbon nanotube microsheet composite prepared via an in situ hydrothermal process. *Electrochim. Acta* **56**, 693–699 (2010)

23. Liu, Y, Mi, CH, Yuan, CZ, Zhang, XG: Improvement of electrochemical and thermal stability of LiFePO₄ cathode modified by CeO₂. *J. Electroanal. Chem.* **628**, 73–80 (2009)
24. Xu, YH, Chen, Y, Wu, J, Li, DC, Ju, H, Zheng, JW: The determination of the kinetic parameters of electrochemical reaction in chemical power sources: a critical review. *Int. J. Hydrogen Energy* **35**, 6366–6380 (2010)

doi:10.1186/2251-6832-4-22

Cite this article as: Ju et al.: Lithium ion intercalation mechanism for LiCoPO₄ electrode. *International Journal of Energy and Environmental Engineering* 2013 **4**:22.

Archive of SID